Brief communication: PICOP, a new ocean melt parameterization under ice shelves combining PICO and a plume model
– Response to reviewers –

Tyler PELLE et al.

January 24, 2019

We thank the two reviewers for their positive and constructive comments that significantly improved the manuscript. While reviewing the manuscript, we found that we used the wrong temperature and salinity input for the Amundsen Sea sector. The correct and updated input for this sector is T $= 0.47^{\circ}$C and S $= 34.73$ psu. As such, we ran PICOP with the correct input and updated the figures and text accordingly. In Fig. 1, we updated the Pine Island ice shelf graphics that show the blank ice shelf with the input, T_a, S_a, and $\dot{m}$. In Fig. 2, we updated the basal melt rate fields for PICO and PICOP, as well as the shelf-wide means. The pattern of basal melting near the grounding lines of Pine Island and Thwaites glaciers remained the same; however, melt rates away from the grounding line decreased significantly as a result of decreased overturning. In addition to making this change, we also address the reviewer's remarks below point by point.

1 Reviewer #1

Proper recognition: This paper is presenting a coupling procedure between existing models. As such, and considering that the authors of the original models are not coauthors, I think effort should be made to properly recognize the original model authors. One way to do this would be to cite the original model studies in the abstract. I note that both models are properly cited throughout the paper, but doing this early and upfront will better recognize the original studies.

We agree with the reviewer and have cited both published models in the abstract of the manuscript.

Comparison to R2013: For specific locations, comparison should be done to actual observations, not just glaciological/ satellite-inferred estimates. You refer to them as "observations", but there are existing observations (e.g. APRES) which resolve basal melting better than a continent wide estimate/survey. Even though this is a brief communication, it will not take much space to compare to existing studies.

This is a great point and we agree that our validation of PICOP would benefit from comparison to existing studies. We added additional comparisons in the discussion section.

Plumes coincide with ice velocities: Sometimes it's necessary that in order to overcome technical limitations, decisions must be made which may not be realistically accurate; this is a parameterisation after all. However, there should be some realistic basis to coinciding plumes with high ice velocities. I think this should be explained more in depth. For example, it should be made clear whether the relatively good agreement with Rignot 2013 is because you expect actual plumes (and hence the high velocities and turbulence which drive melt rate) to be located in the region that your parameterisation predicts. That stability can not be achieved with plumes being initiated with high basal slope is disappointing; perhaps other initiation methods you tested could also be mentioned. Essentially what I'm saying is: are you getting the right answer for the wrong reasons, and in which case, would you expect these results to hold for future scenarios with evolving cavity geometry and a different ice velocity. This choice requires more justification and physical reasoning, including when this assumption could be expected to break down.

Physical justification and clarification of the choice to use ice velocities to advect grounding-line heights has been added to the PICOP-methods section. A description of when this assumption is expected to break down has been added to the discussion section.

Technical corrections:
P1L8: capitalisation of Plume is not necessary.

Done.

P1L10: "a wide variety" change to "several." You only showed us 3 regions.

Done.

P1L12: "able to reproduce". What you're referring to is "able to match Rignot et al., 2013", which I think could be more accurately stated by saying "able to reproduce inferred high melt rates beneath"...

We agree and changed the wording of this sentence.

P1L21: periphery OF the AIS

Done.

P1L21-P2L1: long sentence, consider splitting in half.

Done.

P7L2: "better agreement with observation than PICO, because PICOP."

Done.

Figure 1: "on" in green box has mismatched font.

We changed the font in the green box of Fig. 1 to match the other boxes.

Table 1: in the External Quantity section, you have many "-" in the value column. I would change the column header to "Source", and then cite the study where you pull the quantities from e.g. Far-field ocean temperature, etc.

Done. For quantities that are computed by PICOP from the input data, we specify which model component calculates it (either PICO or the plume model).

Table 1: missing ϵ value?

We added ϵ to Table 1.

2 Reviewer #2

A Brief Communication in TC might allow for a more superficial description of the various model components, but to gain a thorough insight the reader is forced to read the original publications of Reese et al. (2018) and Lazeroms et al. (2018). Without doing so, one has to trust that the model set-up is correct, the right parameters have been used, and a realistic forcing is applied.

We believe the text presented is suitable as a Brief Communication in TC because we couple two existing, published models. Both models were implemented into ISSM without alteration (except for the computation of the grounding line height in the plume model, which is described in the

methods section), so we do not think it is necessary to restate the complete setup of both models. Rather, the methods section provides an overview of the two models, guides the reader to the appropriate sections of the original publications, and details the coupling between the two original models. Forcing applied to PICOP was taken from Reese et al. (2018) to facilitate comparison between PICO and PICOP.

The only way left for evaluation is the comparison of basal melt rates (Fig. 5) for three different ice shelf regions at the rim of the Antarctic Ice Sheet. The latter, however, bears some subjectivity and might have tempted the authors to use the term "in excellent agreement". However, first, the authors "only" compare their results with one observation (Rignot et al., 2013), which actually is not an in-situ observation.

We agree that the validation of PICOP would benefit from additional comparison, aside from Rignot et al. (2013). We added more comparisons in the discussion section of the text, including high definition ocean modeling studies and in-situ observations.

It is not obvious to the reader which set of parameters has be used, what tuning has been applied to reach this agreement.

Since both models were implemented without change from the original publications, the full list of parameters that were used to implement PICOP are found in the original publications. There was no tuning applied to PICOP; the only quantities that changed in the computation of the basal melt rate fields for the three basins were the far field ocean temperature and salinity (taken from Reese et al. (2018)).

The agreement for Filchner-Ronne Ice Shelf (FRIS) is difficult to assess since an inappropriate color scale is used. Various approaches show, and the results of Reese et al. (2018) greatly exaggerate, that refreezing occurs below FRIS. I hope it is only a matter of the color scale, since the pattern shows promising.

We agree that the color scale used in Fig. 2 for the Filchner-Ronne Ice Shelf (FRIS) was not appropriate, as it did not show refreezing and was also over-saturated. We changed the color scale for the FRIS from log to linear, changed the color map to reduce saturation, and extended the bounds to include refreezing in gray-scale. We note that PICOP does not model refreezing well due to the lower bound applied to the ambient ocean temperature and highlight it as one of the limitations of PICOP in the discussion section.

Melting at the ice shelf front can also not be resolved by PICOP, since it is a different process which drives this frontal melting.

The reviewer is correct, we removed this sentence from the text that incorrectly described the frontal melt of the FRIS.

Specific comments:
P1L18: The term "upwelling" is not correctly used. In Physical Oceanography, "upwelling" means the vertical displacement of deep water masses towards the surface, caused by the prevailing winds, e.g., at the Antarctic Divergence, off Namibia, etc. Here, it is the spreading of mCDW onto the continental shelf and, sometimes, into the fringing ice shelf cavities.

This is a good point and we changed the manuscript to correctly describe this process.

P2L16: The name might be misleading, but PICO was NOT designed to reproduce the density driven overturning circulation within sub-ice shelf cavities. The latter, however, was the intention of the box model developed by Olbers and Hellmer (2010).

We changed the description to more correctly say that PICO simulates vertical overturning, as was stated in Reese et al. (2018).

P4L03: It is unclear where the ice depth-averaged velocity v is actually coming from – either from the ice-sheet model coupled to PICOP or from observations. In addition, ϵ is not listed in Table 1.

We added clarification at this point in the text; the depth-averaged velocity is taken from the ice-sheet model. We also added ϵ to Table 1.

P4L07: Same for z_b assumed to be taken from Bedmap2.

We added the source of input data to Table 1, which will clarify this to the reader. We also state that we use geometry from Bedmap2 at the beginning of the results section.

P4L27: The assumption that the ambient temperature in the ice shelf cavity T_a is equal or above the surface freezing point is unfortunate, at least for cold cavities like FRIS and Ross Ice Shelf, since the observations show temperatures well below T_f characteristic of Ice Shelf Water. This assumption might lead to an exaggeration of basal melting in these cavities.

We highlight the lower bound applied to the ambient ocean temperature as a limitation of PICOP in the discussion section. We also added a statement about how cold-cavity basal melt rates may be over estimated by PICOP and reference FRIS in Fig. 2.

P5L12: The mean salinity for the Amundsen Sea of 34.86 is wrong, e.g., Dutrieux et al. (2014) and seems to be a transposed digits since 34.68 makes more sense. Such high salinity causes a

stronger overturning circulation and thus higher basal melting. Same for the southern Weddell Sea continental shelf, where a salinity above 34.8 is only observed in the far western corner, which, I have to admit, provides most of the shelf water fueling basal melting underneath Ronne Ice Shelf.

We recognize that these mean salinity values may be in slight disagreement with observations (Dutrieux et al. (2014) reports a mean salinity that is $\sim$0.2 psu lower than our value used for the Amunsen Sea sector). The mean temperature and salinity values used to force PICOP were taken directly from Reese et al. (2018) and we use them for the sake of comparison. In addition, we ran PICOP with a mean salinity of 34.68 psu over the Amundsen Sea sector and found that the small deviation in mean salinity did not have a significant impact on the modeled basal melt rates.

Table 1: Checking the constant parameters used in Reese et al. (2018) one realizes that they sometimes differ from those used for PICOP, which leaves the impression that Table 1 shows a mixture of parameters used in the original models. In addition, the overturning strength C used in Reese et al. (2018) – Table 1 was a best-fit, which does not necessarily mean that a strength of 1×10^6 is also the best choice for PICOP. Finally, please explain why most units include $^\circ$C but the "freezing point-depth coefficient."

We reorganized Table 1 to group constant parameters that are common to both of the original publications and those that are unique to each publication. We recognize that the overturning strength is a best-fit value for PICO and there may be a more appropriate value for PICOP. However, we use 1×10^6 in our study for the sake of comparison between PICOP and PICO. Lastly, we changed the units for the freezing point-depth coefficient to include $^\circ$C rather than K.

Technical corrections:
P1L01: "basal melt" is the liquid resulting from ocean induced ice shelf "basal melting" – please use the latter term.

Done.

P1L11 - and the following: The term Filchner-Ronne Ice Shelf is widely recognized, e.g. in Reese et al. (2018).

We changed the name of this ice shelf from Ronne-Filchner to Filchner-Ronne in the text.

P1L21: "... along the periphery OF the AIS...."; sentence too long, split in two.

Done.

P3L08: Temperature T and salinity S are already used for the far field temperature and salinity. I suggest omitting "with temperature T, and salinity S".

170 Done.

171 *P7L21: "... are projected to change within the coming century, ... " needs a reference.*

172 Done.

References

Dutrieux, P., De Rydt, J., 1 Jenkins, A., Holland, P., H.K., H., Lee, S., Steig, E., Ding, Q., Abrahamsen, E., and Schröder, M.: Strong Sensitivity of Pine Island Ice Shelf Melting to Climatic Variability, Science, 343, 174–178, https://doi.org/10.1126/science.1244341, 2014.

Lazeroms, W. M. J., Jenkins, A., Gudmundsson, G. H., and van de Wal, R. S. W.: Modelling present-day basal melt rates for Antarctic ice shelves using a parametrization of buoyant meltwater plumes, The Cryosphere, 12, 49–70, https://doi.org/10.5194/tc-12-49-2018, 2018.

Reese, R., Albrecht, T., Mengel, M., Asay-Davis, X., and Winkelmann, R.: Antarctic sub-shelf melt rates via PICO, The Cryosphere, 12, 1969–1985, https://doi.org/10.5194/tc-12-1969-2018, 2018.

Rignot, E., Jacobs, S., Mouginot, J., and Scheuchl, B.: Ice shelf melting around Antarctica, Science, 341, 266–270, https://doi.org/10.1126/science.1235798, 2013.

Brief communication: PICOP, a new ocean melt parameterization under ice shelves combining PICO and a plume model

Tyler Pelle[1], Mathieu Morlighem[1], and Johannes H. Bondzio[1]

[1]University of California, Irvine, Department of Earth System Science, Irvine, CA 92697-3100, USA

Correspondence: Tyler Pelle (tpelle@uci.edu)

Abstract. Basal ~~melt~~ melting at the bottom of Antarctic ice shelves is a major control on glacier dynamics, as it modulates the amount of buttressing that floating ice shelves exert onto the ice streams feeding them. Three-dimensional ocean circulation numerical models provide reliable estimates of basal melt rates but remain too computationally expensive for century scale projections. Ice sheet modelers therefore routinely rely on simplified parameterizations either based on ice shelf depth or on more sophisticated box models. However, existing parameterizations do not accurately resolve the complex spatial patterns of sub-shelf melt rates that have been observed over Antarctica's ice shelves, especially in the vicinity of the grounding line, where basal ~~melt~~ melting is one of the primary drivers of grounding line migration. In this study, we couple the Potsdam Ice-shelf Cavity mOdel ~~(PICO)~~ (PICO, Reese et al., 2018) to a buoyant ~~Plume~~ plume melt rate parameterization (Lazeroms et al., 2018) to create PICOP, a novel basal melt rate parameterization that is easy to implement in transient ice sheet numerical models and produces a melt rate field that is in excellent agreement with the spatial distribution and magnitude of observations for ~~a wide variety of~~ several ocean basins. We test PICOP on the Amundsen Sea sector of West Antarctica, Totten and Moscow University ice shelves in Eastern Antarctica, and the ~~Ronne-Filchner ice shelf~~ Filchner-Ronne Ice Shelf and compare the results to PICO. We find that PICOP is able to reproduce ~~the~~ inferred high melt rates ~~near the grounding lines of~~ beneath Pine Island, Thwaites, and Totten glaciers (on the order of 100 m/yr) and removes the "banding" pattern observed in melt rates produced by PICO over the ~~Ronne-Filchner ice shelf~~Filchner-Ronne Ice Shelf. PICOP resolves many of the issues contemporary basal melt rate parameterizations face and is therefore a valuable tool for those looking to make future projections of Antarctic glaciers.

1 Introduction

Glaciers around the periphery of the Antarctic Ice Sheet (AIS) have undergone dynamic changes due to the ~~upwelling~~ spreading of warm modified Circumpolar Deep Water (mCDW) onto the continental shelf and, sometimes, into sub-ice shelf cavities (e.g., Jacobs et al., 2011; Pritchard et al., 2012). This process drives enhanced basal ~~melt~~melting, which has the potential to reduce the buttressing effect that ice shelves exert on grounded ice upstream (e.g., Rignot and Jacobs, 2002). ~~As this upwelling~~ This spreading of mCDW is expected to increase along sectors of the periphery of the AIS due to the poleward intensification of

the Southern Hemisphere westerly winds (Dinniman et al., 2012). As such, accurately parameterizing these basal melt rates is necessary in making future projections of the AIS due to the large computational cost of two way ice-ocean model coupling. Many early basal melt rate parameterizations (i.e., parameterizations based on the local heat flux at the ice-ocean interface (DeConto and Pollard, 2016; Beckmann and Goosse, 2003) or on basal slopes (Little et al., 2012)) do not accurately capture the impact of ocean circulation within sub-shelf cavities, which is a key control of basal melting. Two of the most recently published melt parameterizations that resolve sub-shelf ocean circulation are the Potsdam Ice-shelf Cavity mOdel (PICO, Reese et al., 2018) and one based on the physics of buoyant ~~meltwater plumes (Plume model, Lazeroms et al., 2018)~~melt water plumes (plume model, Lazeroms et al., 2018). Although both parameterizations are novel in their own regards, melt rates calculated by PICO suffer from unrealistic "banding" as a product of its box model approach and remain too low near grounding lines. In addition, the ~~Plume~~ plume model requires complete sub-shelf ocean temperature and salinity fields as inputs, and has not been adapted to use in transient model runs. We overcome these limitations by combining both PICO and the ~~Plume~~ plume model to form PICOP: we rely on PICO's box model to reconstruct the temperature and salinity fields beneath ice shelves based on far field ocean properties and then use this reconstruction to drive the ~~Plume~~ plume model, which calculates the basal melt rate field. In this brief communication, we describe the physics used to derive PICOP and compare melt rates produced by PICO and PICOP to observations by Rignot et al. (2013) in three basins of varying oceanic conditions and geometry.

2 Methods

2.1 PICO

PICO is a two-dimensional sub-shelf melt rate parameterization that ~~was designed to reproduce the density driven overturning circulation within~~ simulates vertical overturning in sub-shelf cavities and is used here to produce ambient ocean temperature and salinity fields (Reese et al., 2018). Inputs for PICO are the basin-averaged ocean temperature T and salinity S and sub-shelf ocean circulation is driven by the *ice pump* mechanism (Lewis and Perkin, 1986). Individual mesh elements or grid cells within the model domain are assigned a box number based on their relative distance from both the grounding line and ice front. In general, PICO solves for the transport of heat and salt between boxes in contact with the base of the ice shelf, starting at the grounding line and ending at the ice front (boxes $\mathrm{B_k}$ for k = $\{1,\ldots,n\}$, where n is typically less than or equal to 5). After simplification and assuming steady state conditions, the balance of heat and salt in all boxes along the base of the ice shelf can be written as:

$$\begin{aligned} q\,(T_{k-1} - T_k) - A_k m_k \frac{\rho_i}{\rho_w}\frac{L}{c_p} &= 0 \\ q\,(S_{k-1} - S_k) - A_k m_k S_k &= 0. \end{aligned} \tag{1}$$

Using a simplified formulation of the 3-equation melt model by Holland and Jenkins (1999), the transport equations can be solved for salinity S_k and temperature T_k in box $\mathrm{B_k}$, and are dependent on the local pressure p_k, the box area A_k, and the temperature T_{k-1} and salinity S_{k-1} of the upstream box $\mathrm{B_{k\text{-}1}}$. The strength of the overturning circulation, q, is calculated once

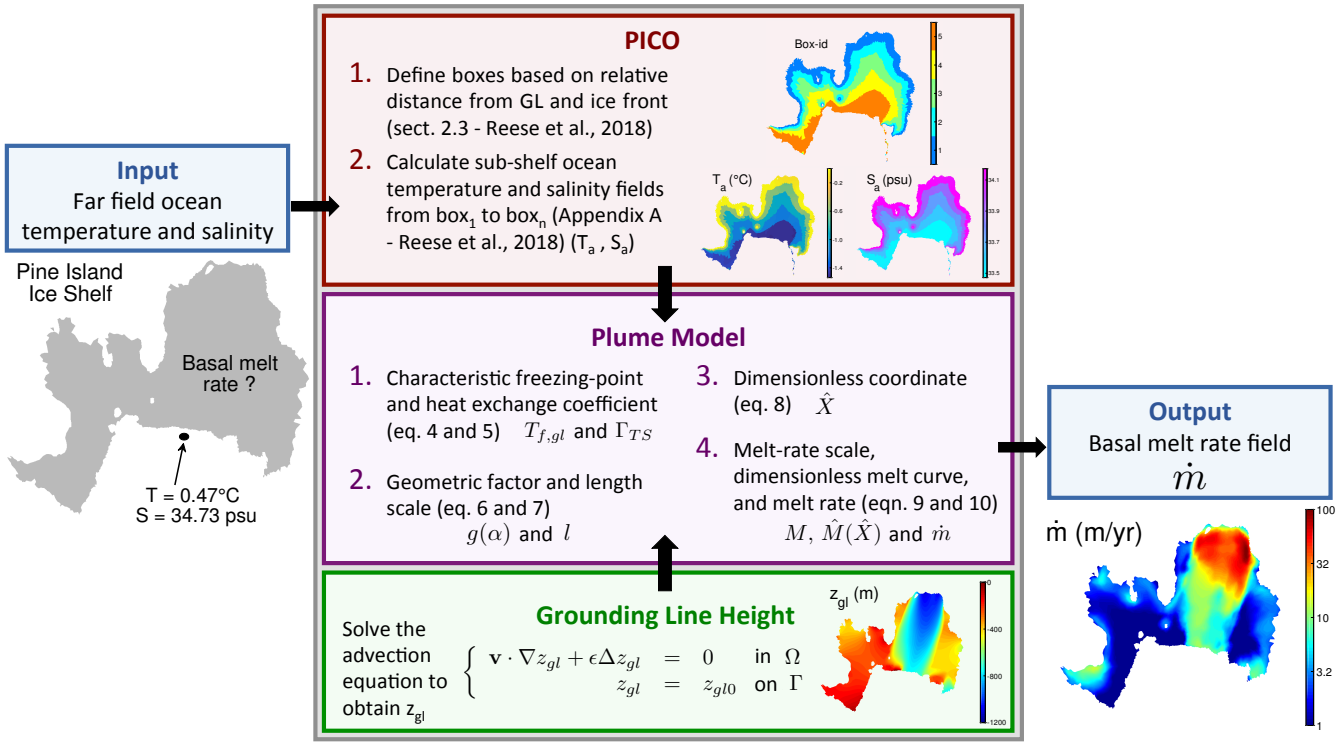

Figure 1. Schematic diagram of PICOP with example data displayed for the Pine Island ice shelf of West Antarctica. The inputs into the parameterization are the basin averaged ocean temperature (°C) and salinity (psu), which are first fed into PICO (red box). PICO uses these inputs to calculate the sub-shelf ambient ocean temperature and salinity fields, which are then used in the ~~Plume~~ plume model (purple box). In addition, the grounding line height is calculated at this time by solving the advection problem defined in the green box. Once these three fields are fed into the ~~Plume~~ plume model, the basal melt rate field is computed according to the steps outlined in the purple box.

per time-step in box B_1 from the density difference between the far field and grounding line water masses:

$$q = C(\rho_0 - \rho_1). \tag{2}$$

Here, we do not use PICO's melt rate parameterization but only use the sub-shelf temperature and salinity fields to drive the ~~Plume~~ plume model (Fig. 1). All constants and external parameters referenced in this paper are summarized in Table 1. For a full derivation of PICO, see Reese et al. (2018).

2.2 Plume model

The ~~Plume~~ plume model is a basal melt rate parameterization based on the theory of buoyant melt water plumes that travel upward along the base of the ice shelf from the grounding line to the location where the plume loses buoyancy. The two-dimensional formulation from Lazeroms et al. (2018) is adapted from the one-dimensional plume model developed by Jenkins (1991) for a plume traveling in direction X ~~with temperature T, and salinity S~~ in an ocean with ambient temperature T_a and

salinity S_a (provided by PICO). We begin by defining the grounding line depth, z_{gl}, over the entire ice shelf, as it is necessary to determine where individual plumes originate in order to employ this parameterization. As a first approximation, we solve an advection equation:

$$\begin{cases} \mathbf{v} \cdot \nabla z_{gl} + \epsilon \Delta z_{gl} = 0 & \text{in } \Omega \\ z_{gl} = z_{gl0} & \text{on } \Gamma \end{cases} \tag{3}$$

where z_{gl0} is the grounding line depth defined at the grounding line Γ, Ω is the ice shelf, and as a first approximation, $\mathbf{v}$ is the ~~ice~~ modeled, depth-averaged ice velocity. Note that ϵ is a small diffusion coefficient introduced to minimize noise and to provide numerical stability. We ~~therefore make the assumption that melt water plumes coincide with ice velocities. We~~ attempted using other advection schemes, for example based on basal slopes, but the level of noise made these approaches unpractical. As such, we make the assumption that the source of individual melt water plumes coincide with ice velocity. If areas of ice convergence and divergence on a shelf are neglected, we generally expect for ice-shelf thickness to decrease as we move from the grounding line to the ice front. Since melt water plumes are driven by buoyancy, it is then reasonable to assume that for small ice shelves, the average trajectory of a plume would be from the grounding line to the ice front. As such, using the ice velocity in the advection scheme to approximate the depth at which the plume originated is not an unreasonable assumption as a first approximation. For larger ice shelves however, sub-shelf flow is affected by different mechanisms that cannot be captured by a simplified parameterization, such as polynya variability. Note that for any given point x on the base of an ice shelf, the grounding line height $z_{gl}(x)$ associated with that point only describes where the plume originated; it does not say anything about the path of the plume from $z_{gl}(x)$ to x.

In a second step, we correct z_{gl} such that, if z_{gl} is greater than the height of the base of the ice shelf, z_b, then we set $z_{gl} = z_b$. Compared to the algorithm used to determine z_{gl} in Lazeroms et al. (2018), advecting grounding line heights is computationally more efficient for higher resolution model runs because we do not have to search for multiple possible plume sources at every point within a given ice shelf.

Now that z_{gl} is defined, we continue by computing both the characteristic freezing point $T_{f,gl}$ and the effective heat exchange coefficient Γ_{TS} as follows:

$$T_{f,gl} = \lambda_1 S_a + \lambda_2 + \lambda_3 z_{gl} \tag{4}$$

$$\Gamma_{TS} = \Gamma_T \left(\gamma_1 + \gamma_2 \frac{T_a - T_{f,gl}}{\lambda_3} \times \frac{E_0 \sin\alpha}{C_d^{1/2} \Gamma_{TS_0} + E_0 \sin\alpha} \right). \tag{5}$$

A geometric scaling factor $g(\alpha)$ and length scale l are defined in order to give the plume model the proper geometry dependence and scaling according to the distance traveled along the plume path. The scaling factor and length scale are

computed as follows:

$$g(\alpha) = \left(\frac{\sin\alpha}{C_d + E_0 \sin\alpha}\right)^{1/2} \left(\frac{E_0 \sin\alpha}{C_d^{1/2}\Gamma_{TS} + E_0 \sin\alpha}\right)^{1/2} \left(\frac{E_0 \sin\alpha}{C_d^{1/2}\Gamma_{TS} + E_0 \sin\alpha}\right) \tag{6}$$

$$l = \frac{T_a - T_{f,gl}}{\lambda_3} \times \frac{x_0 C_d^{1/2}\Gamma_{TS} + E_0 \sin\alpha}{x_0 \left(C_d^{1/2}\Gamma_{TS} + E_0 \sin\alpha\right)}. \tag{7}$$

The dimensionless scale factor x_0 used in the second term of l defines the transition-point between melting and refreezing and is constant for all model results. For a complete explanation of the individual terms that make up these two factors, see section 2.2 of Lazeroms et al. (2018).

The length scale is then used in the computation of the dimensionless coordinate, $\hat{X}$:

$$\hat{X} = \frac{z_b - z_{gl}}{l}. \tag{8}$$

Note that $\hat{X} = 0$ corresponds to the position of the grounding line and $\hat{X} = 0.56$ is the aforementioned transition point, but $\hat{X} = 1$ does not necessarily correspond to the position of the calving front due to the dependence of $\hat{X}$ on l. In order to ensure valid values of $\hat{X}$, we set a lower bound for the ambient ocean temperature: $T_a \geq \lambda_1 S_a + \lambda_2$. The melt rate $\dot{m}$ is then calculated as

$$\dot{m} = \hat{M}(\hat{X}) \times M, \tag{9}$$

where $\hat{M}(\hat{X})$ is a dimensionless melt curve defined in Lazeroms et al. (2018) and M is defined as

$$M = M_0 \times g(\alpha) \times \left(T_a - T_f\left(S_a, z_{gl}\right)\right)^2. \tag{10}$$

For a full derivation of the buoyant plume model used in PICOP, see Lazeroms et al. (2018).

3 Results and Discussion

We evaluate PICOP using geometry from Bedmap2 (Fretwell et al., 2013) and far field ocean temperature and salinity values averaged at the depth of the continental shelf between 1975 to 2012 (Reese et al., 2018; Schmidtko et al., 2014). Here, we compare the modeled basal melt rates calculated by PICO and PICOP to melt rates inferred from conservation of mass and satellite interferometry (Rignot et al., 2013), that we refer to as "observations". Additionally, we compare the modeled basal melt rate field of select ice shelves to in-situ observations and regional modeling studies. We focus on three regions: the Amundsen Sea sector of the West Antarctic Ice Sheet, the Totten and Moscow University ice shelves of the East Antarctic Ice Sheet, and the ~~Ronne-Filchner ice shelf~~Filchner-Ronne Ice Shelf (FRIS). Model inputs for these basins are (~~1.04~~0.47°C, ~~34.86~~ 34.73 psu), (−0.73°C, 34.73 psu), and (−1.76°C, 34.82 psu), respectively.

The spatial distribution of melt rates produced by PICOP is in significantly better agreement with observations compared to PICO, especially in the vicinity of the grounding line where accurate melt rates are needed in order to correctly capture the

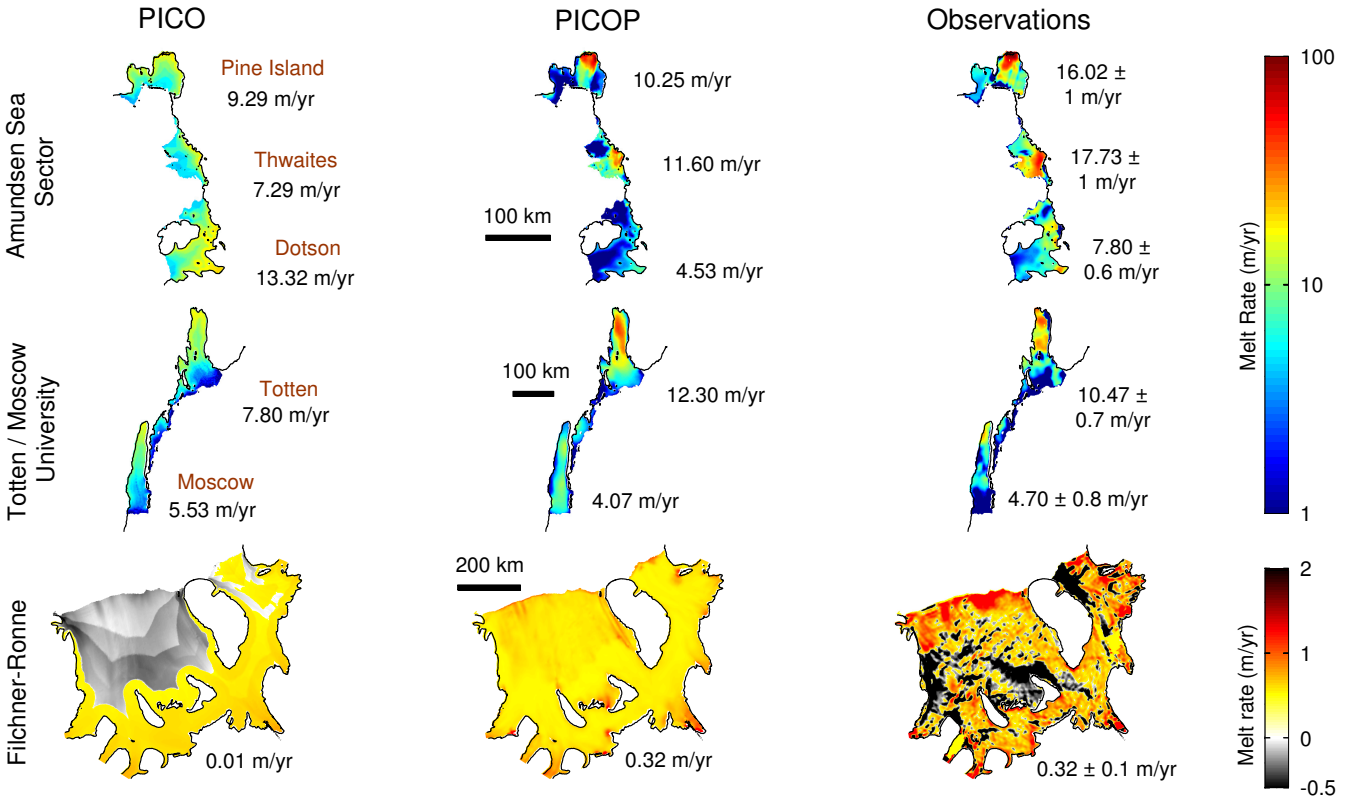

Figure 2. Modeled (PICO and PICOP) and observed (Rignot et al., 2013) melt rates (m/yr) are displayed for the Amundsen Sea sector of West Antarctica (including Pine Island, Thwaites, and Dotson ice shelves), Totten and Moscow University ice shelves of East Antarctica, and the ~~Ronne-Filchner ice shelf~~FRIS. Note that the upper colorbar (Amundsen Sea sector, Totten, and Moscow University) is in log-form while the lower colorbar (FRIS) is linear. Numerical values under PICO and PICOP are area weighted mean melt rates. The observed annual mean melt rate is displayed under the observed melt rate panel.

glacier's grounding line dynamics. In Fig. 2, we see that modeled melt rates produced by PICOP reach approximately ~~100~~ 100 m/yr and 70 m/yr near the grounding line of Pine Island and Thwaites glaciers, respectively, as compared to approximately ~~40~~ 20 m/yr by PICO. These high melt rates are a product of the deeply entrenched bed that both Pine Island and Thwaites glaciers are grounded to. These bed depths are advected with the modeled ice velocity when z_{gl} is solved for, leading to high melt rates that better match observations. Melt rates modeled by Dutrieux et al. (2013), constrained by high resolution satellite and

airborne observations of ice surface velocity and elevation, show melt rates on the order of 100 m/yr near Pine Island glacier's grounding line and 30 m/yr a short 20 km downstream. This sharp gradient in the melt rate field was reproduced by PICOP and will certainly have a major impact on the ice dynamics of this glacier.

A similar situation occurs under Totten ice shelf; melt rates modeled by PICOP reach a maximum of about ~~50~~ 50 m/yr, while those from PICO reach a maximum of approximately ~~20~~ 20 m/yr. Simulated melt rates by Gwyther et al. (2014) show a similar pattern of melt, with basal melt rates of approximately 50 m/yr computed near the upstream most portion of both Totten and Moscow University's grounding lines. Modeling these high melt rates is especially important in ~~the upstream-most portion~~ this region of Totten's grounding line, ~~where~~ as complex grounding line retreat has been observed over the past 17 years and has been found to be strongly sensitive to changes in ocean temperature (Li et al., 2015). Over the ~~Ronne-Filchner ice shelf~~FRIS, the inherent geometry dependence of PICOP reduced the "banding" that modeled melt rates from PICO displayed. This is a significant improvement because as can be seen in Fig. 2, there is a very sharp gradient in the melt rate field computed by PICO over the ~~Ronne-Filchner ice shelf~~ FRIS that would lead to unrealistic ice-shelf dynamics in transient model runs. PICOP produces a smooth transition from high to low melt rates that better matches observations. ~~Additionally, significant melt was computed near the ice front of this ice shelf~~Shelf-wide basal melt rate fields computed by three dimensional ocean - ice shelf coupled models (e.g., Timmermann et al., 2012) show maximum melting (4.5 - 7 m/yr) near the deepest sectors of the grounding line of Ronne glacier, agreeing well with PICOP. Site specific observations (e.g., Jenkins et al., 2010) show a decrease in basal melting to less than 1 m/yr near the Kroff ice rise, which is ~~a product of the high slopes that PICOPconsiders when computing melt rates~~also reproduced by PICOP.

In all three basins, area-weighted mean melt rates calculated with PICOP show ~~significantly~~ better agreement with Rignot et al. (2013). The values reported in figure two corresponding to PICO differ from those used in figure 5 of Reese et al. (2018) because we model these basins using a significantly higher mesh resolution (minimum element size of ~~500~~ 500 m, maximum of ~~10~~ 10 km). By modeling Totten, Pine Island, and Thwaites ice shelves with a coarse mesh, only two boxes were defined for these smaller shelves in Reese et al. (2018), and thus, a larger proportion of the ice shelf was modeled as the ~~grounding-line~~ grounding line box. Melt rates computed in this box are the highest across the shelf because no heat has been lost from the ocean water by the addition of cold melt water, leading to higher mean melt rates when compared to those displayed in figure 2. By using a finer mesh to evaluate PICOP, we are able to capture the fine details of the melt pattern, which are key in predicting the evolution of grounding line dynamics, as well as maintain shelf-averaged melt rates that are in relatively good agreement with observations. The mean melt rates ~~of Pine Island , Thwaites, and Totten~~ for Pine Island and Thwaites ice shelves are ~~slightly overestimated (18.92~~ underestimated (10.25 m/yr ~~, 20.70~~ and 11.60 m/~~yr and 12.30 m/~~yr, respectively), as calculated melt rates are too low away from the vicinity of the grounding line. In addition, the mean melt rate for Totten ice shelf is slightly overestimated (12.30 m/yr) when modeled with PICOP due to the strong grounding line advection used to compute z_{gl} in ~~these regions~~this region. Over the ~~Ronne-Filchner ice shelf~~FRIS, PICOP models a shelf-mean melt rate that is in better agreement with ~~observation than PICOdoes~~ observations than PICO, because PICOP produces melt further downstream of the grounding line as a result of its geometry dependence. In this sector of the ice shelf, PICO primarily computes refreezing ($\dot{m} < 0$), which drives the mean melt rate down to ~~0.01~~ 0.01 m/yr.

While PICOP resolves many of the issues displayed in contemporary sub-shelf mate rate parameterizations, it is limited by the assumptions that were made when both PICO and the ~~Plume~~ plume model were originally derived (see Reese et al. (2018) and Lazeroms et al. (2018)). In addition, when computing z_{gl}, we ~~assume that melt water plumes travel in the same direction as the ice velocity rather than in the direction of~~ assumed that the ~~greatest basal slope. In doing so, we inevitably consider erroneous plume paths that lead to inconsistencies in the computed melt rate fields.~~depth of the plume origin at any point on an ice shelf could be found by following the flow of velocity upstream to the grounding line. Although a good first approximation, we expect this assumption to fail in zones of complex basal geometry (i.e. areas of convergent and divergent ice flow) that would lead melt-water plumes to follow more convoluted paths. We also expect this assumption to fail in large sub-shelf cavities, such as under the FRIS or Ross ice shelf, where plume paths are influenced by processes not captured by this parameterization (i.e. sea ice and polynya variability, the Coriolis Effect that produces a clockwise sub-shelf ocean circulation, and tides). Finally, PICOP does not model refreezing well in cold basins due to the lower limit imposed on the ambient ocean temperature. The ocean temperature output from PICO in cold basins (i.e. the ~~Ronne-Filchner~~ FRIS and Ross ice ~~shelves~~shelf) falls below this lower bound, especially in the vicinity of the ice front, where the coldest ocean temperatures are modeled. As such, melt rates computed in the coldest cavities might be over estimated and cannot be further improved unless this constraint is relaxed, as discussed in Appendix A of Lazeroms et al. (2018). This is exemplified in the modeled basal melt rates produced by PICOP in Fig. 2. Observations show patches of refreezing under the FRIS that are not resolved by PICOP as a result of this lower temperature bound. Yet, PICOP remains an accurate and computationally efficient melt rate parameterization that can be easily implemented into high resolution, transient ice sheet numerical models.

4 Conclusions

Here, we presented a new basal melt rate parameterization that is a combination of both PICO and a ~~Plume~~ plume model. By utilizing PICO to resolve the sub-shelf ocean circulation and produce ambient ocean temperature and salinity fields, we reduce model inputs to only basin-averaged values. Additionally, the geometry dependence of the ~~Plume~~ plume model produces melt rates that show better agreement with observations in terms of both spatial distribution and magnitude than with PICO alone. ~~As ocean~~ Ocean induced melting has been cited as a major driver of change for Antarctic glaciers and ~~because~~ over the coming century, enhanced spreading of mCDW onto the continental shelf is expected as Southern Ocean conditions are projected to change ~~within the coming century~~(Dinniman et al., 2012). As such, the improvements to the spatial distribution and magnitude of modeled melt rates produced by PICOP, as well as the computational efficiency of this parameterization, offer a valuable tool to more accurately make future projections of Antarctic glaciers.

Code and data availability. The data used in this study are freely available on the National Snow and Ice Data Center, or upon request to the authors. ISSM is open source and freely available at http://issm.jpl.nasa.gov.

Author contributions. TP developed the idea of combining PICO and a plume model, and implemented it into ISSM with help from MM and JB. All authors participated in the writing of the manuscript.

Competing interests. None

Acknowledgements. This work was performed at the University of California Irvine under a contract with the National Aeronautics and Space Administration, Cryospheric Sciences Program (#NNX15AD55G).

Table 1. ~~Constants~~ Constant parameters and external quantities referenced in this communication. Common parameters are those used in the derivation of both PICO and the plume model. Unique parameters are from the derivation of the plume model, except for the overturning strength, which was taken from PICO. See Reese et al. (2018) and Lazeroms et al. (2018) for a full list of constants used to derive PICOP.

~~External Quantity~~ **External Quantity**	~~Symbol~~ **Symbol**	
Far-field ocean temperature	T	~~–~~Rees
Far-field ocean salinity	S	~~–~~Rees
~~Ambient ocean temperature T_a - °C Ambient ocean temperature S_a - PSU~~ Local depth of ice shelf base	z_b	~~–~~Fretwe
Local slope angle	α	~~–~~Geometry from Fretwe
Grounding line depth	z_{gl}	~~–~~Solve adve
Ambient ocean temperature	T_a	
Ambient ocean salinity	S_a	
Basal melt rate	$\dot{m}$	
~~Constant Parameter~~ **Common Constant Parameters**	~~Symbol~~ **Symbol**	
Gravitational acceleration	g	
Density of ice	ρ_i	
Density of sea water	ρ_w	
Latent heat of fusion	L	
Heat capacity of sea water	c_p	
Unique Constant Parameters	**Symbol**	
Overturning strength	C	
Entrainment coefficient	E_0	
Drag coefficient	C_d	
Turbulent heat exchange coefficient	$C_d^{1/2}\Gamma_T$	
Freezing point-salinity coefficient	λ_1	
Freezing point offset	λ_2	
Freezing point-depth coefficient	λ_3	
Melt-rate parameter	M_0	
Heat exchange parameter	$C_d^{1/2}\Gamma_{TS_0}$	
Heat exchange parameter	γ_1	
Heat exchange parameter	γ_2	
~~Dimentionless~~ Dimensionless scaling factor	x_0	
Epsilon	ϵ	

References

Beckmann, A. and Goosse, H.: A parameterization of ice shelf–ocean interaction for climate models, Ocean Modelling, 5, 157–170, 2003.

DeConto, R. and Pollard, D.: Contribution of Antarctica to past and future sea-level rise, Nature, 531, 591–597, https://doi.org/10.1038/nature17145, 2016.

Dinniman, M., Klinck, J., and Hofmann, E.: Sensitivity of circumpolar deep water transport and ice shelf basal melt along the west Antarctic Peninsula to changes in the winds, J. Oceanogr., 25, 4799–4816, https://doi.org/10.1175/JCLI-D-11-00307.1, 2012.

Dutrieux, P., Vaughan, D. G., Corr, H. F. J., Jenkins, A., Holland, P. R., Joughin, I., and Fleming, A. H.: Pine Island glacier ice shelf melt distributed at kilometre scales, Cryosphere, 7, 1543–1555, https://doi.org/10.5194/tc-7-1543-2013, http://www.the-cryosphere.net/7/1543/2013/, 2013.

Fretwell, P., Pritchard, H. D., Vaughan, D. G., Bamber, J. L., Barrand, N. E., Bell, R., Bianchi, C., Bingham, R. G., Blankenship, D. D., Casassa, G., Catania, G., Callens, D., Conway, H., Cook, A. J., Corr, H. F. J., Damaske, D., Damm, V., Ferraccioli, F., Forsberg, R., Fujita, S., Gim, Y., Gogineni, P., Griggs, J. A., Hindmarsh, R. C. A., Holmlund, P., Holt, J. W., Jacobel, R. W., Jenkins, A., Jokat, W., Jordan, T., King, E. C., Kohler, J., Krabill, W., Riger-Kusk, M., Langley, K. A., Leitchenkov, G., Leuschen, C., Luyendyk, B. P., Matsuoka, K., Mouginot, J., Nitsche, F. O., Nogi, Y., Nost, O. A., Popov, S. V., Rignot, E., Rippin, D. M., Rivera, A., Roberts, J., Ross, N., Siegert, M. J., Smith, A. M., Steinhage, D., Studinger, M., Sun, B., Tinto, B. K., Welch, B. C., Wilson, D., Young, D. A., Xiangbin, C., and Zirizzotti, A.: Bedmap2: improved ice bed, surface and thickness datasets for Antarctica, Cryosphere, 7, 375–393, https://doi.org/10.5194/tc-7-375-2013, 2013.

Gwyther, D. E., Galton-Fenzi, B. K., Hunter, J. R., and Roberts, J. L.: Simulated melt rates for the Totten and Dalton ice shelves, Ocean Sci., 10, 267–279, https://doi.org/10.5194/os-10-267-2014, 2014.

Holland, D. and Jenkins, A.: Modeling thermodynamic ice-ocean interactions at the base of an ice shelf, J. Phys. Oceanogr., 29, 1787–1800, 1999.

Jacobs, S. S., Jenkins, A., Giulivi, C. F., and Dutrieux, P.: Stronger ocean circulation and increased melting under Pine Island Glacier ice shelf, Nat. Geosci., 4, 519–523, https://doi.org/10.1038/NGEO1188, 2011.

Jenkins, A.: A one-dimensional model of ice shelf-ocean interaction, J. Geophys. Res., 96, 20 671–20 677, 1991.

Jenkins, A., Nicholls, K. W., and Coor, H. F. J.: Observation and Parameterization of Ablation at the Base of Ronne Ice Shelf, Antarctica, J. Phys. Oceanogr., 40, 2298–2312, https://doi.org/10.1175/2010JPO4317.1, 2010.

Lazeroms, W. M. J., Jenkins, A., Gudmundsson, G. H., and van de Wal, R. S. W.: Modelling present-day basal melt rates for Antarctic ice shelves using a parametrization of buoyant meltwater plumes, The Cryosphere, 12, 49–70, https://doi.org/10.5194/tc-12-49-2018, 2018.

Lewis, E. and Perkin, R.: Ice Pumps And Their Rates, J. Geophys. Res., 91, 1756–1762, 1986.

Li, X., Rignot, E., Morlighem, M., Mouginot, J., and Scheuchl, B.: Grounding line retreat of Totten Glacier, East Antarctica, 1996 to 2013, Geophys. Res. Lett., 42, 8049–8056, https://doi.org/10.1002/2015GL065701, 2015.

Little, C. M., Goldberg, D., Gnanadesikan, A., and Oppenheimer, M.: On the coupled response to ice-shelf basal melting, J. Glaciol., 58, https://doi.org/10.3189/2012JoG11J037, 2012.

Pritchard, H. D., Ligtenberg, S. R. M., Fricker, H. A., Vaughan, D. G., van den Broeke, M. R., and Padman, L.: Antarctic ice-sheet loss driven by basal melting of ice shelves, Nature, 484, 502–505, https://doi.org/10.1038/nature10968, 2012.

Reese, R., Albrecht, T., Mengel, M., Asay-Davis, X., and Winkelmann, R.: Antarctic sub-shelf melt rates via PICO, The Cryosphere, 12, 1969–1985, https://doi.org/10.5194/tc-12-1969-2018, 2018.

Rignot, E. and Jacobs, S.: Rapid bottom melting widespread near Antarctic ice sheet grounding lines, Science, 296, 2020–2023, https://doi.org/10.1126/science.1070942, 2002.

Rignot, E., Jacobs, S., Mouginot, J., and Scheuchl, B.: Ice shelf melting around Antarctica, Science, 341, 266–270, https://doi.org/10.1126/science.1235798, 2013.

Schmidtko, S., Heywood, K., Thompson, A., and Aoki, S.: Multidecadal warming of Antarctic waters, Science, 346, https://doi.org/10.1126/science.1256117, 2014.

Timmermann, R., Wang, Q., and Hellmer, H.: Ice-shelf basal melting in a global finite-element sea-ice/ice-shelf/ocean model, Ann. Glaciol., 53, 303–314, https://doi.org/10.3189/2012AoG60A156, 2012.